Substituted biurets as uranophilic ligands: a facile DMSO-induced conversion of a 1:1 into a 2:1 uranyl–ligand complex

Kevin T. Potts*, James J. O'Brien and **Fook S. Tham**
Department of Chemistry, Rensselaer Polytechnic Institute, Troy, NY 12180-3590 (U.S.A.)

(Received April 13, 1990)

Abstract

1,5-Bis[6-(1-ethoxycarbonyl-3-thioureido)-2-pyridindiyl]biuret and uranyl acetate gave a crystalline 1:1 uranyl–ligand complex which, on crystallization from DMSO, underwent rearrangement to a crystalline 2:1 uranyl–ligand complex and a stoichiometric amount of the uncomplexed ligand. Spectral characteristics of these ligands and their uranyl complexes together with single crystal X-ray data for the uranyl–ligand complexes are described.

Introduction

The most effective ligating atoms for the uranyl ion have been shown to be oxygen, nitrogen and sulfur with their efficiencies decreasing in that order [1–6]. The majority of the uranophilic ligands studied to date incorporate oxygen and/or nitrogen as the ligating atoms with only a few examples described where sulfur behaves in this fashion. These ligating atoms are usually part of simple bidentate ligands such as 2,2′-bipyridyl and phenanthroline, or open-chain, macrocyclic, and polymeric polydentate systems such as Schiff bases, azines, 1,3-diketones, ureas, carboxylic acid derivatives and dithiocarbamates [1–13]. The resultant uranyl–ligand complexes possess a wide range of stability constants, with the largest (log $K_f = 18$–19) reported recently for calixarene derivatives [14] (Fig. 1).

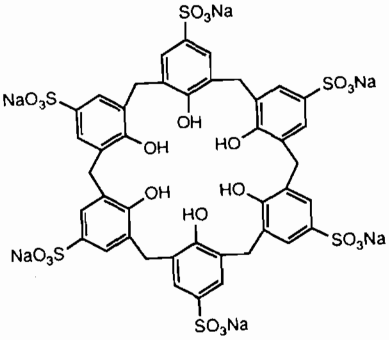

Fig. 1. A uranophilic calixarene derivative.

The carbonyl group appears frequently in these ligands and has shown a high affinity for the uranyl ion. X-ray data of uranyl ion complexes show that the favored arrangement of donor atoms is equatorial or pseudo-equatorial with five to seven, generally six, ligating atoms arranged in this equatorial plane. These X-ray data show [7, 8, 15–17] that the normal binding cavity has a diameter between 4.7 and 5.2 Å.

Our interest in the design and synthesis of uranophilic ligands has led us to study the uranyl binding properties of carbonylureas and biuret derivatives. In such functional groups, the hardness of the ligating atoms is enhanced over analogous 1,3-diketones by the incorporation of nitrogen atoms which also bear labile protons and facilitate the conversion of these groups into their conjugate bases. Hückel molecular orbital calculations show that both the carbonylurea and biuret groups, on conversion to their anions, have essentially the same net charge density on the oxygen donor atoms and an enhanced hard character (HOMO β-stabilization) when compared to that of a 1,3-diketonate ion. In other studies with carbonylthioureas we have found that they readily complex transition metals, adopting a pseudo-square planar geometry about the metal center with the two sulfur atoms *cis* to each other. Ease of synthesis, purification and high yields of metal complexes suggested that the incorporation of this functional group linked with the biuret moiety would afford an effective binding system for the uranyl ion.

---

*Author to whom correspondence should be addressed.

0020-1693/90/$3.50

Experimental

Spectral characterizations were carried out on the following instrumentation: infrared spectra, Perkin-Elmer model 298 and/or 337 infrared spectrophotometer; ^{1}H NMR spectra, Varian T-60, XL-200 and/or Perkin-Elmer R600 spectrometer with TMS as an internal standard; mass spectra, Hewlett-Packard GC/MS System model 5987A; UV–Vis spectra, Varian Cary 219 spectrophotometer. Melting points were determined in capillaries on a Thomas-Hoover capillary melting point apparatus or a Mel-temp apparatus and are uncorrected. Microanalyses were performed by Atlantic Microlab Inc., Atlanta, GA or Robertson Laboratory, Inc., Madison, NJ. Evaporations were carried out under reduced pressure using a rotatory evaporator. Anhydrous solvents were prepared as follows: tetrahydrofuran was treated with potassium hydroxide, then distilled over metallic sodium; acetone was dried over 4 Å Linde molecular sieves and then distilled; toluene was stored over metallic sodium and decanted. Ethoxycarbonyl isocyanate and ethoxycarbonyl isothiocyanate were prepared by literature procedures [18, 19].

Ligand synthesis and complexation

1-(6-Amino-2-pyridindiyl)-3-ethoxycarbonylurea (2)

A solution of freshly distilled ethoxycarbonyl isocyanate (8.00 g, 6.96×10^{-2} mol) in anhydrous tetrahydrofuran (40 ml) was added over 1 h to a stirred solution of 2,6-diaminopyridine (7.59 g, 6.96×10^{-2} mol) in tetrahydrofuran (200 ml) under N_2. Stirring was continued at ambient temperature for 15 h when a portion of the solvent (200 ml) was removed by evaporation, and the remaining slurry was then quenched in ice and water (500 ml) with vigorous stirring. The precipitate was collected, dissolved in a minimum volume of aqueous hydrochloric acid (5% wt./wt.) and, after filtration, the filtrate was neutralized with aqueous sodium hydroxide (50% wt./wt.) The precipitated product was collected, washed with ample water, dried in air, and crystallized from a minimum volume of hot ethanol affording colorless, irregular prisms: 13.74 g (88%); m.p. 340 °C (dec.); IR (KBr) ν(NH) 3460, 3300 cm^{-1}, ν(CO) 1610 cm^{-1}; ^{1}H NMR (200 MHz, DMSO-d$_6$) δ 10.53 (s, 1, NH), 10.03 (s, 1, NH), 7.43 (t, 1, aromatic), 7.14 (d, 1, aromatic), 6.20 (d, 1, aromatic), 6.03 (s, 2, NH_2), 4.23 (q, 2), 1.26 (t, 3); mass spectrum, *m/z* (relative intensity) 224 (M^+, 43), 178 (5), 135 (65), 109 (100). *Anal.* Calc. for $C_9H_{12}O_3N_4$: C, 48.21; H, 5.36; N, 25.00. Found: C, 48.30, H, 5.41; N, 24.94%.

1,5-Bis(6-amino-2-pyridindiyl)biuret (3)

Method A. A slurry of 1-(6-amino-2-pyridindiyl)-3-ethoxycarbonylurea (**2**) (5.00 g, 2.23×10^{-2} mol) and 2,6-diaminopyridine (4.86 g, 4.46×10^{-2} mol) in anhydrous toluene (250 ml) was stirred under N_2 and slowly warmed to reflux. After heating the mixture for 50 h, the separated product was collected from the hot reaction mixture and, after drying in air, the product was stirred with water (100 ml), collected and dried. Crystallization from a minimum volume of hot ethanol afforded colorless, irregular prisms of **3**: 5.93 g (93%); m.p. 220–221 °C (dec.); IR (KBr) ν(NH) 3305, 3210 cm^{-1}, ν(CO) 1690 cm^{-1}; ^{1}H NMR (200 MHz, DMSO-d$_6$) δ 10.80 (bs, 1, NH), 10.10 (s, 1, NH), 7.43 (t, 2, aromatic), 6.97 (bd, 2, aromatic), 6.24 (d, 2, aromatic), 6.04 (s, 4, NH_2); mass spectrum, *m/z* (relative intensity) 287 (M^+, 40), 244 (23), 135 (19), 109 (100). *Anal.* Calc. for $C_{12}H_{13}O_2N_7$: C, 50.17; H, 4.53; N, 34.15; Found: C, 50.09; H, 4.57; N, 34.04%.

Method B. A stirred solution of 2,6-diaminopyridine (40.00 g, 3.66×10^{-1} mol) in anhydrous tetrahydrofuran (500 ml) was treated over 1 h at room temperature under N_2 with a solution of freshly distilled ethoxycarbonyl isocyanate (7.50 g, 6.52×10^{-2} mol) in tetrahydrofuran (20 ml). After stirring the reaction mixture for 15 h at ambient temperature, the solvent was evaporated, anhydrous toluene (500 ml) was added, and the resulting slurry was warmed slowly to reflux which was maintained for 48 h. The insoluble material that was collected by filtration of the hot reaction mixture was stirred with hot water (2×500 ml), collected and dried in air. This product was extracted with hot acetone in a Soxhlet apparatus and, after evaporation of the acetone, crystallization of the residue from a minimum volume of hot ethanol afforded colorless irregular prisms: 15.51 g (83%). This product was identical in all respects with that prepared by method A above.

1,5-Bis[6-(3-ethoxycarbonyl-1-thioureido)-2-pyridindiyl]biuret (4)

A stirred slurry of 1,5-bis(6-amino-2-pyridindiyl)biuret (**3**) (3.52 g, 1.23×10^{-2} mol) in anhydrous tetrahydrofuran (150 ml) under N_2 was heated over 30 min with a solution of freshly distilled ethoxycarbonyl isothiocyanate (3.22 g, 2.90 ml, 2.46×10^{-2} mol) in tetrahydrofuran (5 ml) being added dropwise. After the addition was completed, the desired product separated from the homogeneous reaction mixture and was collected after the reaction mixture was stirred for 20 h. The product was washed with anhydrous tetrahydrofuran (2×50 ml) and dried in air. The material crystallized from a minimum volume of hot ethanol yielding **4** as colorless microneedles: 6.61 g (98%); m.p. 220–224 °C (dec.); IR (KBr) ν(NH) 3380, 3190 cm^{-1}, ν(CO) 1710 cm^{-1}, ν(CS) 1580 cm^{-1}; ^{1}H NMR (200 MHz, DMSO-d_6) δ 12.16 (s, 1, *NH*), 11.67 (bs, 2, *NH*), 10.32 (s, 2, *NH*), 9.62 (s, 1, *NH*), 8.43 (bd, 2, aromatic), 7.92 (t, 2, aromatic), 7.81 (d, 2, aromatic), 4.28 (q, 4), 1.30 (t, 5); mass spectrum, m/z (relative intensity) 550 [$(M+1)^+$, <1.0], 223 (9), 177 (100), 151 (45), 137 (24), 110 (82). *Anal.* Calc. for $C_{20}H_{23}O_6N_9S_2$: C, 43.71; H, 4.19; N, 22.95. Found: C, 43.64; H, 4.25; N, 22.87%.

1,5-Bis[6-(3-ethoxycarbonyl-1-ureido)-2-pyridindiyl]biuret (5)

1,5-Bis(6-amino-2-pyridindiyl)biuret (**3**) (1.00 g, 3.48×10^{-3} mol) in anhydrous tetrahydrofuran (125 ml) was treated dropwise over 1 h with a solution of freshly distilled ethoxycarbonyl isocyanate (0.80 g, 6.97×10^{-3} mol) in tetrahydrofuran (50 ml), the reaction mixture being stirred vigorously under N_2. Stirring was continued at ambient temperature for an additional 20 h, and the separated product was collected, washed with ample acetone (50 ml) and dried in air. The solid was stirred with aqueous hydrochloric acid (50 ml, 1.0 M), filtered, and the filter cake washed with water (100 ml), hot acetone (50 ml) and dried in air. Crystallization from a minimum volume of hot ethanol afforded **5** as colorless, irregular prisms: 1.64 g (91%); m.p. 235 °C (dec.); IR (KBr) ν(NH) 3250, 3140 cm^{-1}, ν(CO) 1710 cm^{-1}; ^{1}H NMR (200 MHz, DMSO-d_6) δ 10.64 (s, 1.7, *NH*), 10.32 (s, 1.9, *NH*), 10.23 (s, 2.0, *NH*), 9.73 (s, 0.9, *NH*), 4.26 (q, 4.0), 1.24 (t, 5.6). *Anal.* Calc. for $C_{20}H_{23}O_8N_9\cdot H_2O$: C, 44.86; H, 4.67; N, 23.55. Found: C, 45.06; H, 4.38; N, 23.92%.

1-{6-[1-Ethoxycarbonyl-O^1)-3-(thioureato-(1-)-N^2)]-2-(pyridindiyl-N)}-5-[6-(1-ethoxycarbonyl-3-thioureido)-2-pyridindiyl]-[biureato-(1-)-N^2O^2](pyridine-N)dioxouranium(VI) (7)

A solution of 1,5-bis[6-(1-ethoxycarbonyl-3-thioureido)-2-pyridinyl)biuret (**4**) (1.00 g, 1.82×10^{-3} mol) in pyridine (100 ml) and powdered uranyl diacetate dihydrate (0.78 g, 1.83×10^{-3} mol) was warmed with vigorous stirring until it was homogeneous. After clarification of the solution by filtration, it was stirred for 48 h at ambient temperature. The precipitated orange–red complex was collected and dried in air. Crystallization from a minimum volume of hot pyridine afforded orange–red prisms of **7**: 1.52 g (79%); m.p. 310 °C (dec.); IR (KBr) ν(NH) 3380, 3190, 2980 cm^{-1}, ν(CO) 1705, 1642 cm^{-1}, ν(UO) 925 cm^{-1}; ^{1}H NMR (200 MHz, DMSO-d_6) δ 12.51 (s, 1, *NH*), 12.27 (s, 1, *NH*), 11.94, (s, 1, *NH*), 11.74 (s, 1, *NH*), 10.83 (s, 1, *NH*), 9.04 (d, 1, aromatic), 8.63 (m, 5, aromatic), 8.42 (d, 1, aromatic), 8.12 (q, 2, aromatic), 7.80 (m, 2, aromatic), 7.42 (m, 4, aromatic), 7.20 (d, 1, aromatic), 4.90 (q, 2), 4.32 (q, 2), 1.57 (t, 2), 1.34 (t, 2). *Anal.* Calc. for $C_{20}H_{21}O_8N_9S_2U\cdot 3$pyridine: C, 39.85; H, 3.42; N, 15.94. Found: C, 40.46; H, 3.40; N, 16.08%.

Bis(dimethylsulfoxide-O-1-{6-[1-(ethoxycarbonyl-O^1)-3-(thioureato-(1)-N^1)]-2-(pyridindiyl-N)}-5-{6-[1-(ethoxycarbonyl-O^1)-3-(thioureate-(1-)-N^2)]-2-(pyridindiyl-N)}-[biureato-(2-)-N^1,N^2,O^1,O^2]-bis[dioxouranium(VI)] (8)

A solution of 1-{6-[1-ethoxycarbonyl-O^1)-3-(thioureato-(1-)-N^2)]-2-(pyridindiyl-*N*)}-5-[6-(1-ethoxycarbonyl-3-thioureido)-2-pyridindiyl]-[biureato-(1-)-N^2O^2]-(pyridine-*N*)dioxouranium(VI) (**7**) (0.80, 8.93×10^{-4} mol) in dimethyl sulfoxide (15 ml) was treated with freshly distilled ethyl acetate (100 ml) and after filtration, the reaction mixture was set aside for 48 h. The separated orange needles were collected and dried in air: 0.48 g (86%); m.p. 190 °C (dec.); IR (KBr) ν(UO) 925 cm^{-1}, ν(SO) 945 cm^{-1}; ^{1}H NMR (200 MHz, DMSO-d_6) δ 11.53 (s, 1, *NH*), 11.39 (s, 1, *NH*), 11.08 (s, 1, *NH*), 8.99 (d, 1, aromatic), 8.75 (d, 1, aromatic), 8.14 (m, 2, aromatic), 7.39 (d, 1, aromatic), 7.29 (d, 1, aromatic), 4.89 (q, 2), 4.77 (q, 2), 2.5 (m, 12), 1.53 (m, 6). *Anal.* Calc. for $C_{20}H_{19}O_{10}N_9S_2U_2\cdot 2$DMSO: C, 23.08; H, 2.50; N, 10.17. Found: C, 22.54; H, 2.47; N, 10.34%.

Methods

Analytical procedures used in our studies of these uranyl complexes were the continuous variation method [20–23] (see Fig. 4), the mole ratio method [20, 21] (see Fig. 5), conductometric titration [20, 21] (see Fig. 6), and thermogravimetric analysis (see Fig. 7) for the uranyl–ligand complex (**7**), and thermogravimetric analysis (see Fig. 9) for the uranyl–ligand complex (**8**).

Crystal data for 7: $C_{35}H_{36}N_{12}O_8S_2U_1$, $M=1054.9$, space group $P\bar{1}$ (*No.* 2) $a=12.748(2)$, $b=12.778(2)$, $c=13.916(2)$ Å, $\alpha=64.89(1)$, $\beta=83.80(1)$, $\gamma=89.54(1)°$, $V=2038.8(6)$ Å^3, $Z=2$, $D_{\mathrm{calc}}=1.72$ g/cm^3, crystal size $=0.05\times0.11\times0.36$ mm. Data were collected at room temperature on a Nicolet R3m diffractometer using Mo Kα radiation, $\lambda=0.71069$ Å in an ω-scan mode [ω range: $1.2°+(2\theta(K_{\alpha1})-2\theta(K_{\alpha2}))$]; $2\theta_{\max}=48°$. A total of 6739 reflections was collected of which 5911 were unique and considered observed ($F>3\sigma F$). The programs of SHELXTL (Rev. 5.1) were used for data reduction and other calculations. An empirical absorption correction was applied (μ(Mo) $=39.3$ cm^{-1}). A Patterson map was used to locate the position of the U atom and two cycles of least-squares refinement were used to refine the position of this U atom. A Fourier difference map allowed all 58 non-hydrogen atoms to be recognized. Atomic coordinates and anisotropic temperature factors were refined for all non-hydrogen atoms. Isotropic hydrogen atoms were included in the refinement in calculated positions. The refinements converged at $R=2.53\%$; $R_w=2.54\%$.

Crystal data for **8**: $C_{20}H_{19}N_9O_{10}S_2U_2 \cdot 4.77(C_2H_6SO)$, $M=1458.3$, space group $P2_1/n$ (No. 14), $a=8.538(1)$, $b=32.758(3)$, $c=18.056(2)$ Å, $\beta=101.42(1)°$, $V=4950.2(9)$ Å^3, $Z=4$, D_{calc}, $D_{obs}=1.957$, 1.954 g/cm^3, crystal size$=0.09\times0.17\times0.40$ mm. Data were collected at low temperature (-22 °C) on a Nicolet R3m diffractometer using Mo Kα radiation, $\lambda=0.71069$ Å, in an ω-scan mode [ω range: $1.2°+(2\theta(K_{\alpha1})-2\theta(K_{\alpha2}))$]; $2\theta_{max}=45°$. A total of 7889 reflections was collected of which 5865 were unique and considered observed ($F>3\sigma F$). The programs of SHELXTL (Rev. 5.1) were used for data reduction and all other calculations. An empirical absorption correction was applied (μ(Mo)$=65.3$ cm^{-1}). A Patterson map was used to locate the positions of the U atoms and two cycles of least-squares refinement were used to refine these positions. A Fourier difference map allowed all 63 non-hydrogen atoms to be recognized. Atomic coordinates and anisotropic temperature factors were refined for all non-hydrogen atoms. Isotropic hydrogen atoms were included in the refinement in calculated positions. The refinements converged at $R=4.09\%$; $R_w=4.72\%$.

Results

The synthetic route to the ligand **4** is shown in Fig. 2. Excess 2,6-diaminopyridine (**1**) and ethoxycarbonyl isocyanate in anhydrous THF at room temperature gave an 87% yield of the monoaddition product **2** which underwent condensation with an additional molecule of 2,6-diaminopyridine in refluxing toluene to the 1,5-disubstituted biuret **3** in 83% yield. The intermediate **2** need not be isolated, and details for the direct formation of **3** are given in 'Experimental'. Treatment of **3** with two equivalents of ethoxycarbonyl isothiocyanate in anhydrous THF at room temperature under N_2 gave **4** (LH_7) in 98% yield. The reaction of ethoxycarbonyl isocyanate with **3** likewise gave **5** in 86% yield.

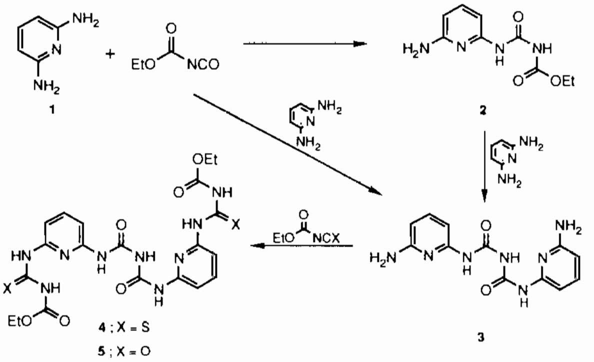

Fig. 2. Reaction sequence for the synthesis of ligands **4** and **5**.

The 1:1 uranyl–ligand complex **7** was obtained from ligand **4** as shown in Fig. 3. Treatment of **4** in methanol with two equivalents of methanolic sodium hydroxide resulted in the dibasic sodium salt **6** (LH_5Na_2), which may be isolated or reacted directly in solution with uranyl acetate. Addition of the methanolic uranyl solution resulted in the immediate precipitation of the orange uranyl–ligand complex **7** (LH_5UO_2). Alternatively the ligand **4**, dissolved in pyridine, may be treated with a solution of uranyl acetate in the same solvent, again giving **7** which crystallizes as orange–red prisms.

Elemental analysis and the analytical procedures shown in Figs. 4–7 established the 1:1 stoichiometry of this complex. In Fig. 4 the UV–Vis absorption spectra for equimolar pyridine solutions of uranyl acetate, the uncomplexed ligand **4**, and the resultant complex **7** are shown in the 300–530 nm region. A strong absorption centered at 346 nm for complex **7** was used to monitor complex formation by the method of continuous variation, the uncomplexed metal salt and ligand exhibiting only weak absorptions at this wavelength. By varying the ligand to metal ratio at constant ionic strength, maximum formation of **7** (maximum absorbance) occurred on approaching a 1:1 ratio of ligand to uranyl. This stoichiometry was established by plotting the absorbance at 346 nm against both the mole fraction and ligand to uranyl ratio of the ligand. The relative formation constant ($K_{rel}=9.04\times10^5$) was obtained by application of these data to the following equation in which A is the maximum absorbance, A_{ext} is the extrapolated absorbance, C is the total concentration, and C_{UO} and C_{LH} are the partial concentrations of uranyl ion and ligand, respectively. The uranyl ion is known to form a relatively stable complex with two acetate anions (UO_2Ac_2) for which the overall stability constant (log β_2) ranges from 4.4 to 4.9 (av.$=4.7$)

$$K_{rel}=\frac{[UO_2LH_5]}{[UO_2^{2+}][LH_7]}$$

$$=\frac{[(A/A_{ext})C]}{[C_{UO_2}-(A/A_{ext})C][C_{LH_7}-(A/A_{ext})C]}$$

$$K_{rel}=9.04\times10^5$$

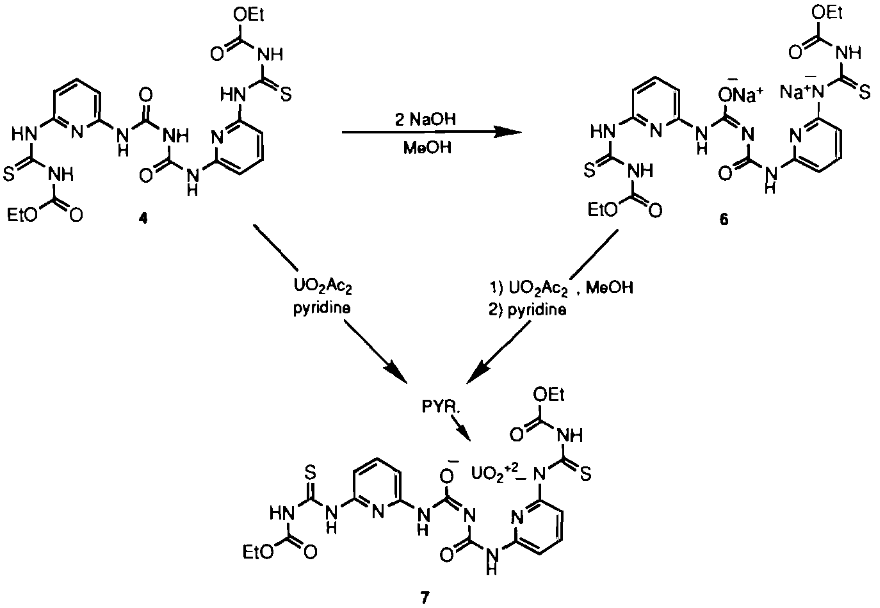

Fig. 3. Synthesis of the 1:1 uranyl–ligand complex 7 from ligand 4.

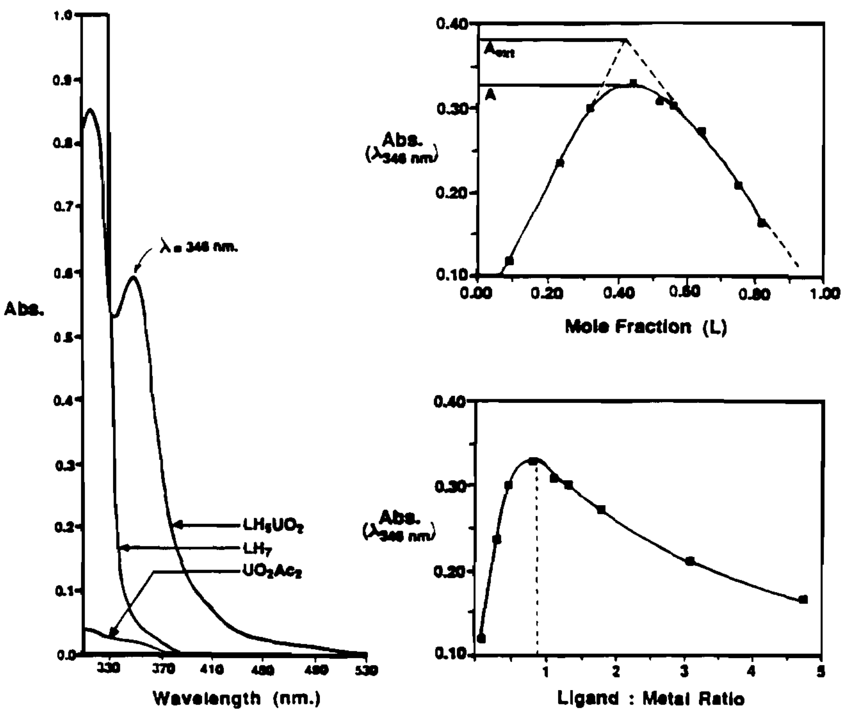

Fig. 4. Continuous variation plots for the 1:1 uranyl–ligand complex 7.

depending on the measurement conditions employed [24–26]. Since the above equation does not account for this association between the uranyl and acetate ions, an estimate of the actual stability constant for the uranyl–ligand complex (log $K_{LH\,UO} = 10.7$) was obtained using the following formula [5, 12].

$$K_{LH_5UO_2} = [K_{rel}][\beta_{UO_2(OAc)_2}]$$

Figure 5 shows the results of applying the mole ratio method in which an acetonitrile solution of the dibasic ligand **6** was titrated with a standard solution of uranyl acetate. The absorbance at 275 nm exhibited by the uncomplexed ligand was monitored and plotted against ligand to metal ratio, and these results are again consistent with 1:1 uranyl–ligand stoichiometry.

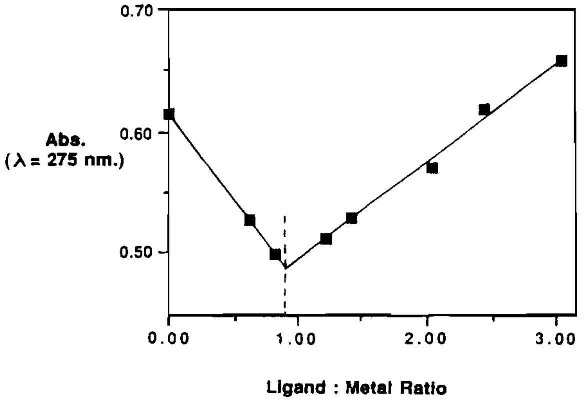

Fig. 5. Mole ratio plot for the 1:1 uranyl–ligand complex 7.

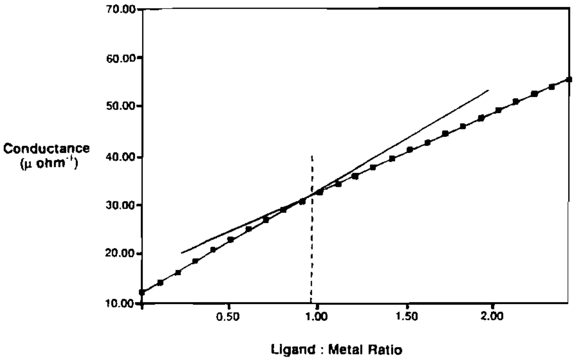

Fig. 6. Conductometric titration plot of UO_2Ac_2 with LH_5Na_2 (6).

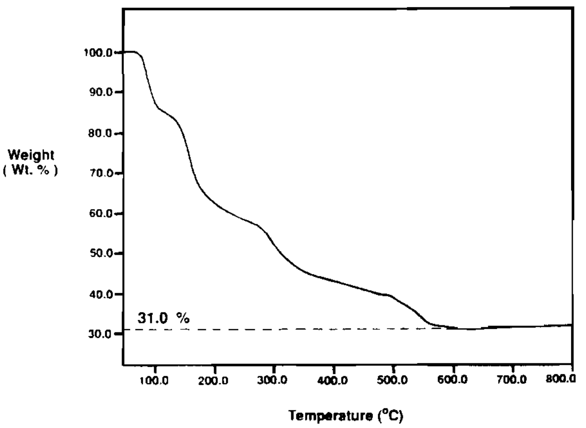

Fig. 7. Thermogravimetric analysis plot for $LH_5UO_2 \cdot Pyr$ (7).

The conductometric titration study is shown in Fig. 6. Conductance was measured in DMF as a solution of uranyl acetate titrated with a standard solution of **6**. The conductance increased steadily during the titration until a 1:1 ratio of ligand to uranyl was reached; beyond this point the conductance increased at a lesser rate. The change in slope at the extrapolated point further substantiates the 1:1 uranyl–ligand stoichiometry. The thermogravimetric analysis curve shown in Fig. 7 shows a weight loss of 69% which represents a thermal degradation of the ligand and solvent portions of the uranyl complex.

Complex **7** was recrystallized from pyridine and combustion analysis indicated an empirical formula of $C_{35}H_{36}O_8N_{12}S_2U$. This composition corresponds to the dibasic ligand, uranyl ion and three pyridines which could not be removed under vacuum without degradation of the crystal structure, suggesting that at least one pyridine is intimately bound in the crystal structure. The single crystal X-ray structure of **7** is shown in Fig. 8.

Dissolution of the 1:1 complex **7** in DMSO, followed by the addition of a large volume of ethyl acetate, resulted in the separation of orange needles which differed from the original prisms which crystallized from pyridine. One equivalent of the original ligand **4** was also obtained from the mother liquor. Thermogravimetric analysis of the air dried complex (Fig. 9) suggested a binding stoichiometry of two uranyl ions per ligand and also indicated the presence of four molar equivalents of DMSO per complex as solvent of crystallization. Combustion analysis for the complex after drying *in vacuo* (0.001 mm Hg, 78 °C) confirmed the 2:1 stoichiometry and indicated the presence of two equivalents of DMSO. The data suggest that of the four DMSO molecules two are simply trapped in the crystal lattice and can be removed while the remaining two are more intimately bound and cannot be removed without degradation of the complex. Figure 10 shows the single crystal X-ray structure of complex **8**.

Ligand **5** was found to bind the uranyl ion similarly to **4** (X = S); however, on treatment with uranyl acetate in pyridine, the 2:1 uranyl–ligand complex **9** was formed directly (Fig. 11) and precipitated by the addition of methanol. There was no evidence for the formation of the 1:1 complex.

Two pyridine molecules were loosely bound in **9** as shown by their facile removal *in vacuo* at ambient temperature without decomposition of the complex. Complex **9** was less stable than the dithio analogue **8** as indicated by the tendency of the ligand to reprotonate in the presence of water resulting in the displacement of the uranyl ion, a function of the lower acidity of carbonylureas relative to analogous carbonylthioureas. The 2:1 uranyl–ligand stoichiometry of **9** was confirmed by its thermogravimetric analysis plot (Fig. 12). A weight loss of 50.66% occurred on heating **9** from 50 to 1000 °C, corresponding to the thermal degradation of the organic

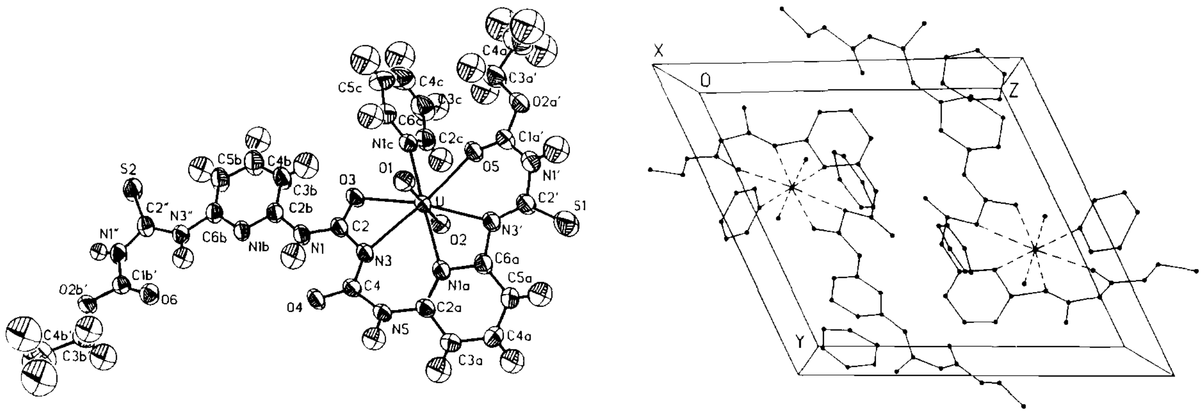

Fig. 8. ORTEP and unit cell plots for complex 7 showing structure and pyridines of crystallization.

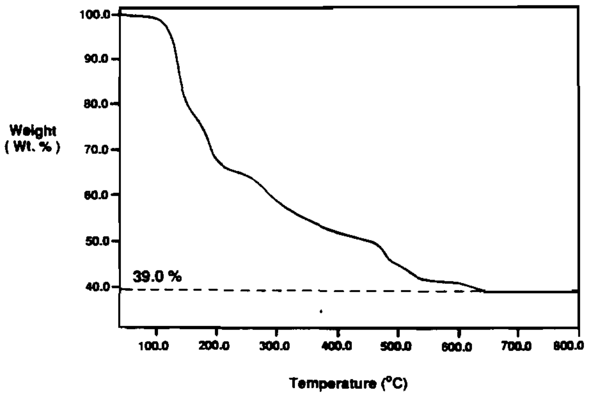

Fig. 9. Thermogravimetric analysis plot for the 2:1 uranyl–ligand complex **8** ($LH_3(UO_2)_2 \cdot 2DMSO$).

portion of the complex containing one part ligand and two parts uranyl ion.

Ligand recovery

Ligands containing the amide or urea moiety show an enhanced stability toward acidic conditions over analogous ligand systems without nitrogen [11], and the ligands **4** and **5** containing biuret and acylurea functionality were found to be quite stable under these conditions. Samples of **4** and **5** were stirred with 1.0 M HCl for an extended period (72 h) at ambient temperature. Isolation of the slurry solids followed by washing (H_2O) and drying (*in vacuo*) afforded 97 and 98% respective recoveries of the ligands which were of high purity (>95%) based on their NMR spectra. When solutions of the purified complexes **7**, **8** and **9** in DMF were stirred with a 0.5 M HCl solution, the immediate loss of orange color indicated the rapid dissociation of the complexes. The freed ligands precipitated and were collected by filtration and, after drying *in vacuo*, resulted in 96 and 98% recoveries of **4** and **5**,

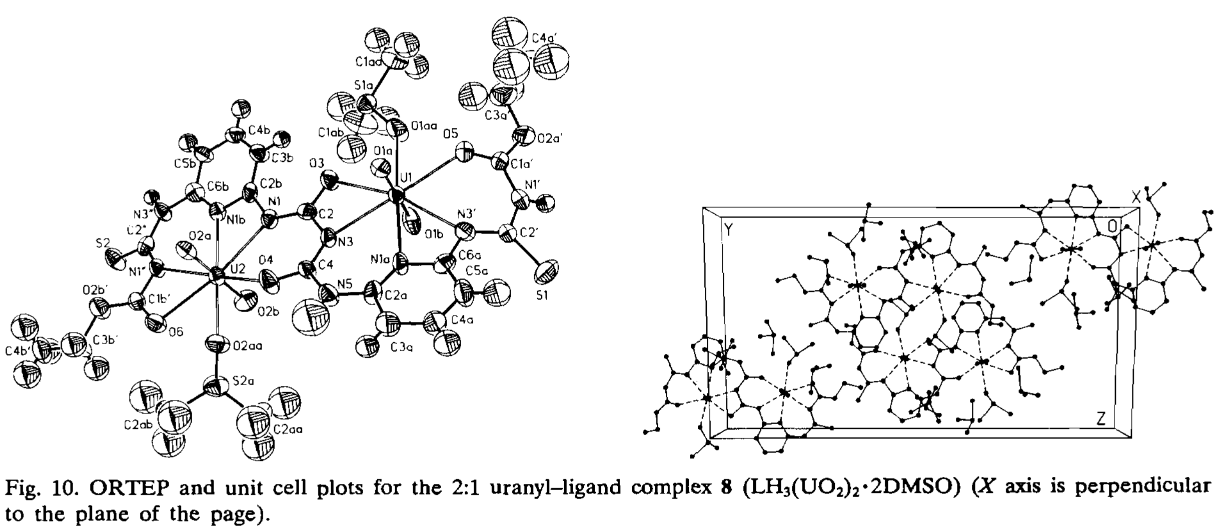

Fig. 10. ORTEP and unit cell plots for the 2:1 uranyl–ligand complex **8** ($LH_3(UO_2)_2 \cdot 2DMSO$) (*X* axis is perpendicular to the plane of the page).

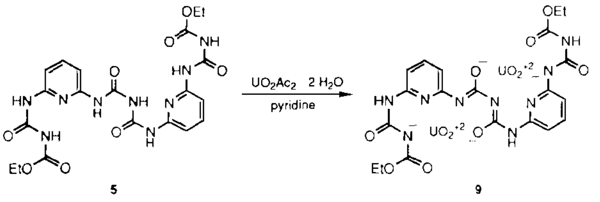

Fig. 11. Direct formation of the 2:1 complex **9** from ligand **5** (X=O).

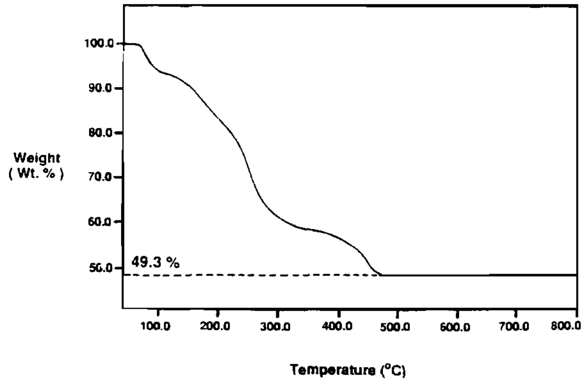

Fig. 12. Thermogravimetric analysis plot for the 2:1 uranyl–ligand complex **9**.

respectively. NMR analysis of the recycled ligands confirmed a high degree of purity (>95%) and the complete removal of the complexed uranyl ions. Subsequent complexations of the recovered ligands have indicated that their uranyl affinities are maintained after recovery.

Discussion

Incorporation of 2,6-pyridindiyl units as rigid, planar bridging groups between the ligating functions enables us to introduce a degree of preorganization to our ligands, as well as provide alternative binding sites. The ligand, 1,5-bis[6-(1-ethoxycarbonyl)-3-thioureido)-2-pyridindiyl]biuret (**4**) is of particular interest, containing seventeen potential ligating atoms of which six are oxygen, nine are nitrogen and two are sulfur. Several possible conformations are available for potential uranyl binding in which 5 or 6 donor atoms are aligned equatorially forming cavity diameters of appropriate size, and these binding conformations offer variety in the donor atoms of the coordination sets (e.g. O_4S_2, N_4S_2, N_5O and N_3O_2). These conformations have been modeled [27] and are shown in Table 1, along with cavity diameters and minimized total energies calculated for each conformation.

There are several unique features about the structure of **7**. The ligating atoms, two oxygen and three

TABLE 1. Total energies and cavity diameters for potential binding conformations of LH_7 (**4**)

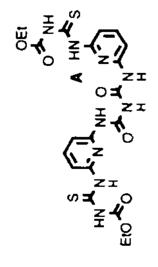 E_{total} = 18.34 kcal Diameter (av.) = 5.28 Å (A), 5.23 Å (B)	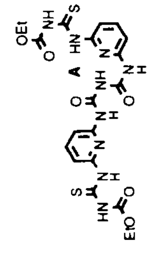 E_{total} = 22.83 kcal Diameter (av.) = 5.35 Å (A)	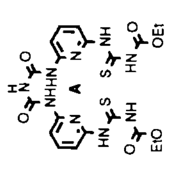 E_{total} = 24.97 kcal Diameter (av.) = 5.50 Å (A)	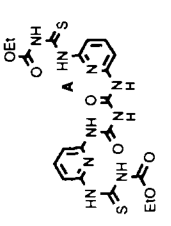 E_{total} = 29.52 kcal Diameter (av.) = 5.58 Å (A)
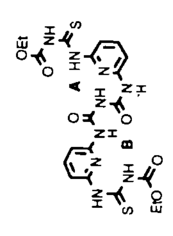 E_{total} = 33.12 kcal Diameter (av.) = 5.40 Å (A)	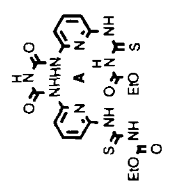 E_{total} = 37.24 kcal Diameter (av.) = 5.26 Å (A)	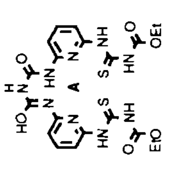 E_{total} = 38.24 kcal Diameter (av.) = 5.47 Å (A)	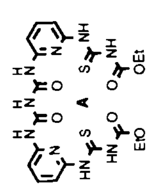 E_{total} = 70.04 kcal Diameter (av.) = 7.24 Å (A)

nitrogen atoms, together with a solvent pyridine nitrogen atom filling the sixth coordination site, all lie in the uranyl equatorial plane, and the solvent pyridine is orthogonal to this plane. The sizes of the rings containing the uranium atom are six-membered (2 rings) and four-membered (2 rings), these rings encapsulating 235° about the uranium atom. Two additional free pyridines of crystallization were evident in the unit cell. It is interesting that of the three potential ligating atoms in **4**, the adjacent nitrogen rather than the 'soft' sulfur was involved in the complexation. The thiocarbonyl group may enhance the acidity of the proton bound to this nitrogen thus facilitating its ionization prior to complexation.

The conversion of the uranyl–ligand complex **7** into complex **8** (Fig. 13) is quite unusual and may be rationalized as follows. The crystalline complex **7** has coordinated pyridine together with pyridine of solvation (eqn. (1)). Dissolution of this complex in DMSO resulted in the coordinated and lattice pyridines being replaced by DMSO, and they were thus available to facilitate ionization of the remaining protons in the $LH_5UO_2 \cdot DMSO$ complex (eqn. (2)). Equilibrium dissociation of the $LH_5 \cdot UO_2 \cdot DMSO$ complex resulted in a small amount of UO_2^{2+} ion in solution available for complexation by the $[LH_3UO_2]^{2-} \cdot DMSO$ species (eqn. (3)). The addition of a large volume of ethyl acetate precipitated this new 2:1 uranyl–ligand complex (**8**, $LH_3(UO_2)_2 \cdot 2DMSO$) from solution as it was formed. Complex **8** may be recrystallized from DMSO without change, and on recrystallization from pyridine, the DMSO was not displaced by pyridine from its coordination sites, demonstrating the high affinity of DMSO for the uranyl ion. It is interesting to note that these complexes form with the ligand conformations that are of the lowest total energies and offer cavities of the most appropriate size for the uranyl ion as predicted by our computer modeling studies. Furthermore, the ligand conformation in **8** is of lower energy than that in **7**, and this reduction of ligand energy may be the impetus for the rearrangement. Intramolecular homobinuclear uranyl complexes are quite rare, and the only other 2:1 uranyl–ligand complexes described are those formed from a heptadentate acyclic Schiff base ligand, ethylenediaminetetraacetic acid derivatives, and polyketonate complexes which contain another metal ion. The synergistic effect of sulfoxides on uranyl complexes is well established with those derived from β-diketones [10, 28–30].

$$LH_7 + UO_2^{2+} + 2AcO^- \xrightarrow{\text{pyridine}}$$

$$LH_5UO_2 \cdot \text{Pyr.} + 2\text{pyridinium acetate} \quad (1)$$

$$2LH_5UO_2 \cdot \text{Pyr.} \xrightarrow{\text{DMSO}} [LH_3UO_2]^{2-} \cdot \text{DMSO}$$

$$+ LH_5UO_2 \cdot \text{DMSO} + 2\text{pyridinium ion} \quad (2)$$

$$[LH_3UO_2]^{2-} \cdot \text{DMSO} + LH_5UO_2 \cdot \text{DMSO} \longrightarrow$$

$$LH_3(UO_2)_2 \cdot 2\text{DMSO} + [LH_5]^{2-} \quad (3)$$

$$[LH_5]^{2-} + 2\text{pyridinium ion} \longrightarrow LH_7 + 2\text{pyridine} \quad (4)$$

Spectral characteristics

Infrared spectra

The infrared spectrum of complex **7** showed a sharp U=O stretching absorption of moderate intensity at 925 cm^{-1}, consistent with reported literature values for this absorption, and two carbonyl group absorptions at 1642 and 1705 cm^{-1}, the former being the more intense absorption. In comparison with the IR spectrum of the ligand **4**, the absorption at 1642 cm^{-1} is new and was assigned to carbonyl groups bound through the oxygen to the uranium. The absorption at 1705 cm^{-1} corresponded to a carbonyl absorption in the ligand, and in the complex it is due to an uncomplexed carbonyl group. Complexity in absorptions between 1300 and 1600 cm^{-1} for the ligand **4** and its uranyl complex **7** unfortunately precluded any definite band assignments in this region. NH absorptions were observed at 3380(s), 3190(b) and 2980(b) cm^{-1} for the ligand, whereas with complex **7** only two absorptions were observed at 3180(b) and 2975(b) cm^{-1}, both being considerably reduced in intensity. Complex **8** showed

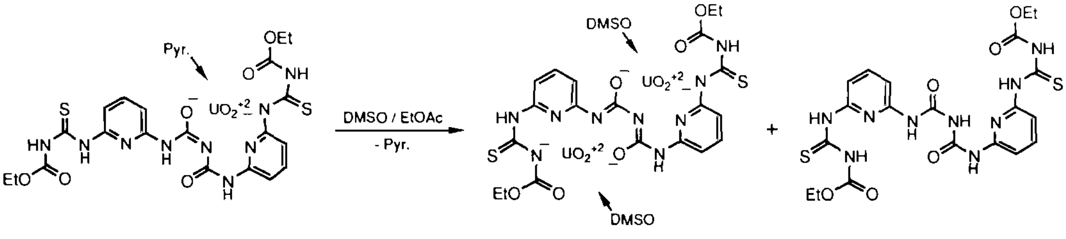

7 8 4

Fig. 13. Rearrangement of the 1:1 complex 7 to the 2:1 complex 8.

a U=O stretching vibration at 925 cm^{-1} and an absorption at 945 cm^{-1} which suggested the presence of bound DMSO. The carbonyl absorption at 1705 cm^{-1} in the pyridine adduct **7** was no longer present and the NH region of the spectrum was broad and poorly defined.

The uncomplexed ligand **5** showed absorptions at 3250, 3140, and 2980 cm^{-1} corresponding to the NH bonds, and at 1705 cm^{-1} for the carbonyl groups. The spectrum of **9** had a single broad NH absorption between 3580 and 2820 cm^{-1}, and the carbonyl absorption was shifted to 1645 cm^{-1}. A strong absorption was observed at 925 cm^{-1} and is characteristic of the uranyl ion.

^{1}H NMR spectra

The ^{1}H NMR spectra (200 MHz, DMSO-d$_6$) of both ligands and complexes were particularly informative for structural purposes. For ligand **4** the ethyl splitting pattern was observed at δ 1.30 (CH$_3$) and 4.28 (CH$_2$); the 3-, 4-, and 5-pyridine ring protons occurred as a doublet at δ 7.81 (J=8 Hz), a triplet at δ 7.92 (J=8 Hz), and a poorly defined doublet at δ 8.43 (J=8 Hz), respectively. The down field shift of the 5-proton relative to the 3-proton (Δ=0.62 ppm) is consistent with this proton being in the deshielding zone of the adjacent thiocarbonyl group, a result of the conformational preference shown by the ethoxycarbonyl thiourea substituent in which the N$_{(3)}$H is hydrogen bonded to the carbonyl oxygen atom. Four distinct NH singlet peaks were observed at δ 9.62 (N$_{(3)}$H of the biuret), 10.32 (N$_{(1)}$H and N$_{(5)}$H of the biuret, 11.67 (N$_{(1)}$H of the thiourea) and 12.16 (N$_{(3)}$H of the thiourea).

On complexation of **4** with the uranyl ion the above NMR spectrum changed significantly. The ethoxycarbonyl thiourea substituents were no longer equivalent, two sets of ethyl groups appearing at δ 1.34 and 1.56 (CH$_3$) and δ 4.32 and 4.90 (CH$_2$). These differences in chemical shifts, when compared to those of the ligand, indicated that one of the ethoxycarbonyl thiourea groups was involved in complexation of the uranyl ion, while the other was not. The chemical shifts of the pyridine protons showed that the two ligand pyridine rings were no longer electronically equivalent and appreciable downfield shifts of the pyridine protons were observed, except for one proton. An enhancement of the spectrum resolution and the observed downfield shifts of these pyridine protons strongly suggest that

TABLE 2. ^{1}H NMR data for LH$_7$ (**4**), LH$_5$UO$_2$·Pyr (**7**) and LH$_3$(UO$_2$)$_2$·2DMSO (**8**)

Compound	Chemical shifts (ppm)					
	N*H*		Aromatic		Ethoxy	
LH$_7$ 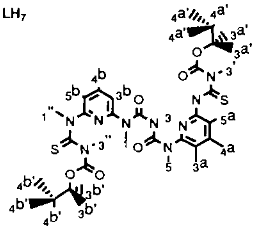	1 3 5 1′ 3′ 1″ 3″	10.32(1) 9.62(1) 10.32(1) 12.16(1) 11.67(1) 12.16(1) 11.67(1)	3a 4a 5a 3b 4b 5b	7.81(1) 7.92(1) 8.43(1) 7.81(1) 7.92(1) 8.43(1)	3a′ 4a′ 3b′ 4b′	4.28(2) 1.30(3) 4.28(2) 1.30(3)
LH$_5$UO$_2$ PYR 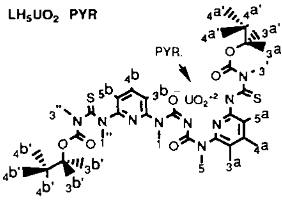	1 3 5 1′ 3′ 1″ 3″	12.51(1) – 10.83(1) – 11.74(1) 12.27(1) 11.78(1)	3a 4a 5a 3b 4b 5b	7.20(1) 8.12(1) 9.04(1) 8.63(1) 8.12(1) 8.42(1)	3a′ 4a′ 3b′ 4b′	4.90(2) 1.56(3) 4.32(2) 1.34(3)
LH$_3$(UO$_2$)$_2$ 2 DMSO 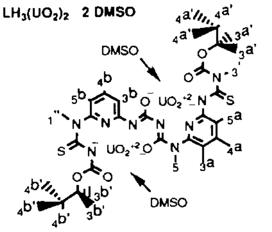	1 3 5 1′ 3′ 1″ 3″	– – 11.07(1) – 11.53(1) 11.39(1) –	3a 4a 5a 3b 4b 5b	7.29(1) 8.14(1) 8.99(1) 8.75(1) 8.14(1) 7.39(1)	3a′ 4a′ 3b′ 4b′	4.89(2) 1.55(3) 4.77(2) 1.52(3)

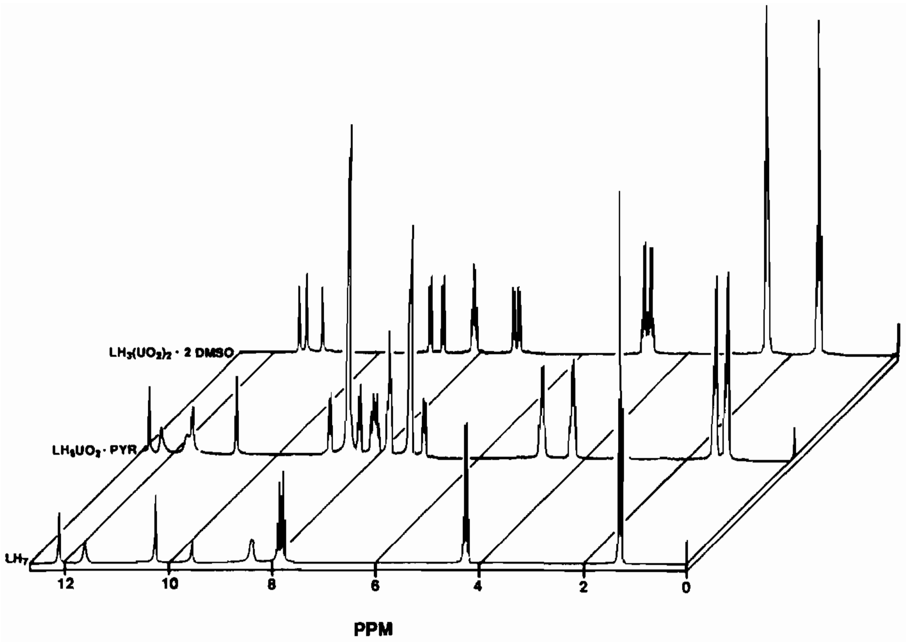

Fig. 14. ^1H NMR spectra of LH_7 (4), LH_5UO_2·Pyr (7) and $LH_3(UO_2)_2$·2DMSO (8).

a nitrogen atom of one pyridine was bound to the uranyl ion.

Five individual NH protons were present as sharp singlets at δ 10.83, 11.74, 11.78, 12.27 and 12.51, each integrating for one proton. This number of non-equivalent NH protons indicated that the ligand complexed as the dianion $[LH_5]^{2-}$, thus forming a neutral but unsymmetrical complex. Combustion analysis indicated the presence of three pyridines of crystallization which were also evident from ^1H chemical shifts at δ 7.43 (m), 7.81 (m) and 8.63 (m).

The ^1H NMR spectrum (200 MHz, DMSO-d_6) of complex **8** was also particularly informative. The presence of bound DMSO in this new complex was shown by a sharp singlet at δ 2.55. The general features of the spectrum indicated that both ethoxycarbonyl thiourea groups were bound to the uranyl ions, but they were not in identical environments. Both pyridine rings were also part of the ligating system and, as there were only three NH resonances (s, 1 H), a tetraanion was involved. The chemical shift assignments for LH_7 (**4**), LH_5UO_2·Pyr (**7**) and $LH_3(UO_2)_2$·2DMSO (**8**) are shown in Table 2, and their spectra are compared in Fig. 14.

The proton ^1H NMR spectrum (200 MHz, DMSO-d_6) of ligand **5** showed chemical shifts at δ 1.24 (t, 6) and δ 4.26 (q, 4) corresponding to the methyl and methylene portions of the two equivalent ethoxy groups, at δ 7.64 (d, 2, $J=8$ Hz), δ 7.69 (d, 2, $J=8$ Hz) and δ 7.83 (t, 2, $J=8$ Hz) corresponding to pyridinyl protons and at δ 9.73 (s, 1), δ 10.23 (s, 2), δ 10.32 (s, 2) and δ 10.64 (s, 2) corresponding to the four sets of non-equivalent acylurea and biuret protons. The ^1H NMR spectrum of its uranyl complex (**9**) had chemical shifts which were generally shifted downfield in an analogous pattern to that observed for complex **8**. Signals corresponding to the two ethoxy groups appeared at δ 1.55 (t, 6) and δ 4.81 (m, 4); the two non-equivalent pyridindiyl units displayed chemical shifts at δ 7.00 (d, 1, $J=8$ Hz), δ 7.21 (d, 1, $J=8$ Hz), δ 8.03 (d, 1, $J=8$ Hz), δ 8.11 (t, 1, $J=8$ Hz), δ 8.39 (t, 1, $J=8$ Hz) and δ 8.71 (d, 1, $J=8$ Hz), and the three remaining NH protons appeared at δ 10.96 (bs, 3).

Supplementary material

Complete X-ray structural data for the ligand–uranyl complexes **7** and **8** are available from Professor K. T. Potts.

Acknowledgements

This work was supported by Department of Energy Research Grant No. DE-FG02-86ER13583, Division of Chemical Sciences, Office of Basic Energy Sciences. We are indebted to Dr R. Kullnig for his guidance in the determination of the X-ray structures and to Professors J. A. Moore and L. V. Interrante for the use of the DTA apparatus.

References

1 H. B. Singh, S. Maheshwari and H. Tomer, *Thermochim. Acta, 64* (1983) 47.
2 R. Monavalen and M. M. Patel, *Makromol. Chem., 184* (1983) 717.
3 S. A. Patil and V. H. Kulkarni, *Inorg. Chim. Acta, 95* (1984) 195.
4 S. Raman, S. C. Shukla and R. S. Thakur, *J. Macromol. Sci. Chem., A17* (1982) 1399.
5 I. Tabushi, Y. Kobuke and A. Yoshizawa, *J. Am. Chem. Soc., 106* (1984) 2481.
6 I. Tabushi, Y. Kobuke and A. Yoshizawa, *J. Am. Chem. Soc., 107* (1985) 4585.
7 N. W. Alcock and D. J. Flanders, *Inorg. Chim. Acta, 94* (1984) 279.
8 N. A. Bailey, S. F. Davison, J. R. Elliot, D. E. Fenton, E. Godbehere, S. K. Holdroyd and C. R. DeBarbarin, *J. Chem. Soc., Dalton Trans.*, (1984) 1073.
9 I. Tabushi, Y. Kobuke and T. Nishiya, *Tetrahedron Lett.*, (1979) 3515.
10 M. S. Subramanian, S. A. Pai and V. K. Manchanda, *Aust. J. Chem., 26* (1973) 85.
11 R. M. Joshi and M. M. Patel, *J. Macromol. Sci. Chem., A19* (1983) 705.
12 I. Tabushi, Y. Kobuke, K. Ando, M. Kishimoto and E. Ohara, *J. Am. Chem. soc., 102* (1980) 5947.
13 R. Marchelli, E. Dradi, A. Dossena and G. Casnati, *Tetrahedron, 38* (1982) 2061.
14 S. Shinkai, H. Koreshi, K. Veda, T. Arimura and O. Manabe, *J. Am. Chem. Soc., 109* (1987) 6371.
15 G. Bandoli, D. A. Glemente, G. Marangoni and G. Paolucci, *J. Chem. Soc., Chem. Commun.*, (1978) 235.
16 G. Bandoli and D. A. Clemente, *J. Inorg. Nucl. Chem., 43* (1981) 2843.
17 E. G. Witte, K. S. Schwochau, G. Henkel and B. Krebo, *Inorg. Chim. Acta, 94* (1984) 323.
18 R. Lamon, *J. Heterocycl. Chem., 6* (1969) 261.
19 R. Lamon, *J. Heterocycl. Chem., 5* (1968) 837.
20 A. A. El-Samahy, A. M. Abdel-Mawgoud, E. A. Abou Gheria and N. M. Ismail, *Bull. Soc. Chim. Fr., 5* (1981) I-175.
21 M. T. El-Haty and F. A. Adam, *Bull. Soc. Chim. Fr., 11* (1983) I-253.
22 P. Job, *Ann. Chim., 10* (1928) 113.
23 D. T. Sawyer, *Chemistry Experiments for Instrumental Methods*, Wiley, New York, 1984.
24 D. D. Perrin, *Stability Constants of Metal–Ion Complexes*, Pergamon, New York, 1979.
25 A. E. Martell, *Stability Constants of Metal–Ion Complexes*, Suppl. 1, The Chemical Society, London, 1971.
26 A. E. Martell, *Stability Constants of Metal–Ion Complexes*, The Chemical Society, London, 1964.
27 *PC Model*, Serena Software, Bloomington, IN 47402-3076, U.S.A.
28 K. Batzar, D. E. Goldberg and L. Newman, *J. Inorg. Nucl. Chem., 29* (1967) 1511.
29 M. S. Subramanian and S. A. Pai, *Aust. J. Chem., 26* (1973) 77.
30 M. S. Subramanian and A. Viswanatha, *J. Inorg. Nucl. Chem., 31* (1969) 2575.